

Thermal Analysis in Railway Electrification Systems for bare conductors

Alejandro Gancedo
CAF Trunkey & Engineering
Zamudio, Bilbao, SPAIN
agancedo@cafte.com

Islam El-Sayed
LEMUR Group
University of Oviedo
islam@uniovi.es

Peru Bidaguren
CAF Trunkey & Engineering
Zamudio, Bilbao, SPAIN
pbidaguren@cafte.com

Pablo Arboleya
LEMUR Group
University of Oviedo
arboleyapablo@uniovi.es

Abstract—This report is based on a Master’s Thesis [1], in which a tool to calculate the thermal behavior of railway electrification systems has been developed by means of iterative calculations based on heat transfer and energy conversion equations. The calculation method is implemented in Matlab, allowing to study the temperature of overhead bare lines. The aim of this tool is to size the section of the conductors (catenary, feeder) and calculate the recovery time of the system against unexpected contingencies. The input data is obtained from RailNeos 2.0, a simulator of railway electrification systems which is able to calculate the total energy consumption of the system, taking into account the implementation of accumulation devices. This tool was developed by Lemur Research Group of the University of Oviedo and CAF Tunrkey & Engineering.

I. INTRODUCTION

Currently, in the electric generation and distribution system, the trend of smart electric networks predominate, where renewable energies and storage systems play a crucial role. At the same time, the need to consolidate a transport system that was capable of moving large masses of passengers and goods, reducing the environmental impact is evident. The road-map foresees that the length of high-speed networks will triple in 2030, covering most of the passengers in middle distance. For transport of goods by road, the 30% will be done by train or ship, in distances greater than 300 km, and more than 50% in 2050 [2].

Foreseeing this encouraging scenario, the stage of design and study of new networks takes a crucial role. Either, power flows and thermal studies allow taking the correct direction of the new network design. A detailed prior study is the first solution to future problems in the grid, what it allows to fulfill the requirements of reliability and profitability expected.

II. TEMPERATURE CALCULATION METHOD

A conductor submitted to voltage and circulating current through it, has a equivalent thermal model. As consequence of the current flowing through the conductor, losses arise due to Joule effect. A flow heat will take place from the wire to the atmosphere. A gradient of temperature will appear, being the main limiting factor of the maximum current without not damaging the components.

This work was partially supported by CAF Turnkey Engineering Company under the grant FUI-024-19 (Railway infrastructure calculations for DC traction networks considering on-board and off-board accumulation systems)

The knowledge of heat transfer and thermodynamic are joined in order to solve thermal problems. The expression of the energy conservation applied to a control volume must be fulfilled for every instant, i.e, a balance in the energy has to exist (see Eq. 1) [3].

$$\underbrace{\frac{dE_{input}}{dt}}_{\dot{E}_{input}} - \underbrace{\frac{dE_{output}}{dt}}_{\dot{E}_{output}} + \underbrace{\frac{dE_{gen}}{dt}}_{\dot{E}_{gen}} = \underbrace{\frac{dE_{stored}}{dt}}_{\dot{E}_{stored}} \quad (1)$$

Eq.1 can be applied to any instant of time and also to an interval of time. The terms \dot{E}_{input} and \dot{E}_{output} are surface phenomena. Conduction, convection and radiation are examples of these surface procedures. The generation term, \dot{E}_{gen} , comes from the conversion of electric to thermal energy following the principle of Joule.

The House and Tuttle [4], with some variations from ECAR [5] is the theorem developed in this report. This thermal calculation method is presented in the standard IEEE Std 738-2012 [6]. It allows to study dynamic problems where the input current is changing over the time. Wind speed and heat solar gain are also taken into account, considering both constants along the simulation. The temperature of the conductors are calculated knowing the power losses.

A. Temperature calculations varying input current and with weather conditions

The increase or decrease in conductor temperature is calculated for each interval of time by means of the heat balance expression which is presented in Eq.2 and Eq.3. The temperature of the previous period is updated with the temperature change.

$$q_c + q_r + m \cdot C_p \cdot \frac{dT_{avg}}{dt} = q_s + \underbrace{I^2 \cdot R(T_{avg})}_{P_{losses}} \quad (2)$$

$$\frac{dT_{avg}}{dt} = \frac{1}{m \cdot C_p} [P_{losses} + q_s - q_c - q_r] \quad (3)$$

B. Convective heat loss

The convective procedure can be split into two groups, natural and forced convection. Natural convection happens when air surrounding the conductor is heated and this mass of air is moved gradually. Forced convection appears when a flow of air is falling upon the conductor and the mass of air is

moved. Natural convection is equivalent to forced convection for speeds lower than 0.2 m/s. The equation presented by McAdams [7] for the calculation of convective heat loss for cylinders will be implemented in this mathematical model.

1) *Forced convection*: In order to distinguish laminar and turbulent flow, House and Tuttle [4] uses two expressions for forced convection. The changing of states is carried out at a Reynolds number equals to 1000 (value calculated as convenience following conductor ampacities). This made that the transition between both states was a discontinuity, instead of a curve as in reality. To avoid the discontinuity, Eq. 4 and Eq. 5 are used. The crosspoint of both curves indicates the transition from laminar to turbulent air flow. Eq. 4 is used for calculating the forced convection at low wind speed and Eq. 5 is employed for forced convection at high wind speed.

$$q_{c1} = K_{angle} [1.01 + 1.35 \cdot N_{Re}^{0.52}] \cdot k_f \cdot (T_s - T_\infty) \quad (4)$$

$$q_{c2} = K_{angle} \cdot 0.754 \cdot N_{Re}^{0.6} \cdot k_f \cdot (T_s - T_\infty) \quad (5)$$

The expression of the wind direction factor is shown in Eq. 6, where ϕ is the angle between the conductor and the wind direction.

$$K_{angle} = 1.194 - \cos(\phi) + 0.194 \cdot \cos(2\phi) + 0.368 \cdot \sin(2\phi) \quad (6)$$

The expression to calculate the dimensionless Reynolds number is shown in Eq. 7.

$$N_{Re} = \frac{D_0 \cdot \rho_f \cdot V_w}{\mu_f} \quad (7)$$

2) *Natural convection*: Natural convection is performed at wind speeds close to zero. In Eq. 8 the expression of the natural convection heat loss is presented.

$$q_{cn} = 3.645 \cdot \rho_f^{0.5} \cdot D_0^{0.75} \cdot (T_s - T_\infty)^{1.25} \quad (8)$$

For low wind speeds, Mc Adams [7] recommends obtaining natural and forced convection heat loss, selecting the most restrictive result. This approach is the one implemented in Matlab.

C. Radiated heat loss

The thermal losses goes from high temperatures to low temperatures, in this case, the energy is transferred from the conductor to the surrounding air. For the thermal study of overhead conductors, Eq. 9 is used.

$$q_r = 17.8 \cdot D_0 \cdot \varepsilon \left[\left(\frac{T_s + 273}{100} \right)^4 - \left(\frac{T_\infty + 273}{100} \right)^4 \right] \quad (9)$$

D. Solar heat gain

The solar heat received for the conductor is calculated with Eq. 10. The heat provided to the conductor leads to an increase on the temperature. The solar heat depends on the solar absorptivity (α), the total solar and sky radiated heat intensity corrected for elevation (Q_{se}), effective angle

of incidence of the sun's rays (θ) and the projected area of conductor (A') in m^2/m , (see Eq. 10).

$$q_s = \alpha \cdot Q_{se} \cdot \sin(\theta) \cdot A' \quad (10)$$

The effective incidence angle of the sun's rays is introduced in Eq. 11.

$$\theta = \arccos[\cos(H_c) \cdot \cos(Z_c - Z_l)] \quad (11)$$

Where, H_c is the altitude of sun (from 0° to 90°), Z_c is the azimuth of sun and Z_l is the azimuth of line.

E. Conductor heat capacity

Conductor heat capacitance results from the product of mass and specific heat per length. In case that several types of material conform the conductor, the total conductor heat capacitance is obtained as sum of the core and the outer edges as it is shown in Eq. 12.

$$m \cdot C_p = \sum m_i \cdot C_{pi} \quad (12)$$

F. Air characteristics, solar angle and solar heat flux

For Natural and Forced heat convection loss, the coefficient of thermal conductivity of air (k_f), air density (ρ_f) and air viscosity (μ_f) are calculated at the average temperature of the boundary layer (T_{film}), see Eq. 13.

$$T_{film} = \frac{T_s + T_\infty}{2} \quad (13)$$

1) *Dynamic viscosity of air*: Dynamic viscosity is a measure to compute the internal resistance between the molecules of a fluid. It relates the stress or local tension in a fluid in motion with the speed of deformation of the fluid particles [8]. For the calculation of dynamic viscosity of air, Eq. 14 is used.

$$\mu_f = \frac{1.458 \cdot 10^{-6} \cdot (T_{film} + 273)^{1.5}}{T_{film} + 383.4}, \quad (14)$$

[kg/(m · s)] or [(N · s)/m²]

2) *Air density*: The air density depends on the elevation of conductor above sea level (H_e) and air temperature of the external layer of the conductor (T_{film}). Eq. 15 represents the mathematical expression of the air density.

$$\rho_f = \frac{1.293 - 1.525 \cdot 10^{-4} \cdot H_e + 6.379 \cdot 10^{-9} \cdot H_e^2}{1 + 0.00367 \cdot T_{film}} \quad (15)$$

[kg/m³]

3) *Thermal conductivity of air*: The thermal conductivity is a physical property of the materials which measures the capacity of heat conduction, i.e, the capacity of transferring kinetic energy from theirs molecules to others adjacent or to substances in contact [9]. The thermal conductivity of air is calculated taken into account T_{film} (see Eq. 16)

$$k_f = 2.424 \cdot 10^{-2} + 7.477 \cdot 10^{-5} \cdot T_{film} - 4.407 \cdot 10^{-9} \cdot T_{film}^2, [W/(m \cdot ^\circ C)] \quad (16)$$

4) *Altitude of the sun*: The expression of the solar altitude of the sun (H_c) in degrees or radians is presented in Eq. 17. The solar altitude is the angle between the sun's rays and the Earth's horizon (see Fig. 2). The Earth is tilted 23.45° in relation of the solar system plane. The value of H_c changes depending on the time of the day, time of the year and latitude of the location. Those places that are close to the equator have higher solar altitude than regions near to the poles [10].

For obtaining H_c , the latitude of the place, hour angle (ω) and solar declination (δ) must be calculated.

$$H_c = a \sin [\cos(Lat)\cos(\delta)\cos(\omega) + \sin(Lat)\sin(\delta)] \quad (17)$$

The hour angle (ω) is the angle considering 0 degrees at noon time and taking 15 degrees for each hour. For instance, 1PM is $+15^\circ C$ (see Fig. 1).

Fig. 1. Representation of the hour angle (ω) during the day

The solar declination (δ) is the angle between the line Sun-Earth and the plane of Earth's equator (see Fig. 2). The expression of solar declination in degrees is shown in Eq. 18. This equation is valid, either for northern hemisphere (Lat higher than 0) and for southern latitudes (Lat lower than 0).

$$\delta = 23.46 \cdot \sin \left[\frac{284 + N}{365} \cdot 360 \right] \quad (18)$$

Where N is the day of the year, for instance, January 8 is equal to 8. The solstices are on 172 and 355, days in which the sun reaches the maximum north declination ($+23.45^\circ$) or south (-23.45°) with respect to equator.

5) *Azimuth of the sun*: The azimuth of the sun (Z_c) is the angle measured between the cardinal North of the Earth and the projection on the horizon of the celestial body which is being observed (see Fig. 2). The angle is always measured in a clockwise direction. In Eq. 19 is shown the expression of the azimuth in degrees.

$$Z_c = C + \arctan(\chi) \quad (19)$$

The solar azimuth variable is presented in Eq. 20.

$$\chi = \frac{\sin(\omega)}{\sin(Lat) \cdot \cos(\omega) - \cos(Lat) \cdot \tan(\delta)} \quad (20)$$

Where C is the solar azimuth constant which is dependent on the hour angle and the solar azimuth variable. In the table I, the solar azimuth constant values are presented.

6) *Total heat flux density*: The expression of the total heat flux density (Q_s) is introduced in Eq. 22. In this expression the solar altitude in degrees (H_c) and coefficients of the cleanliness atmosphere are used.

$$Q_s = A + B \cdot H_c + C \cdot H_c^2 + D \cdot H_c^3 + \quad (21)$$

$$E \cdot H_c^4 + F \cdot H_c^5 + G \cdot H_c^6 \quad (22)$$

The values of the polynomial coefficients for a clear and an industrial atmosphere as function of H_c are gathered in [1].

TABLE I
VALUES OF SOLAR AZIMUTH CONSTANT (C) IN DEGREES, TAKEN INTO ACCOUNT HOUR ANGLE (ω) AND SOLAR AZIMUTH VARIABLE (χ)

ω in degrees	C if $\chi \geq 0$ degrees	C if $\chi < 0$ degrees
$-180 \leq \omega < 0$	0	180
$0 \leq \omega < 180$	180	360

7) *Elevation correction factor*: The total solar and sky radiated heat intensity corrected for elevation (Q_{se}) is calculated with Eq. 23.

$$Q_{se} = K_{solar} \cdot Q_s, [W/m^2] \quad (23)$$

Where the solar altitude correction factor (K_{solar}) is obtained following Eq. 24

$$K_{solar} = A + B \cdot H_e + C \cdot H_e^2 \quad (24)$$

The value of the coefficients used in Eq. 24 are shown in [1]

G. Emissivity and absorptivity of the conductor

Emissivity (ε) and absorptivity (α) are variables interrelated. Both increasing with time, atmospheric pollution and line operating voltage. The researches [11] and [12] define ε and α in the range of 0.2 and 0.3 for new conductors. Depending on the line voltage and the pollution of the air these factor could increase, reaching 0.7 over the time. Studies from EPRI [6], conclude that values of young conductors are in the range of 0.2 and 0.4, in some occasions this band could grow up to 0.5 and 0.9, depending on the line voltage operation and the amount of particles in the atmosphere.

III. RAILTHERMAL APP

RailThermal app is a program developed with Matlab which uses the equations presented previously. It performs an iterative calculation where an initial temperature and climatological conditions are supposed.

As was commented the input data comes from RailNeos. The power losses of the lines are related to the length of the line. In case a train is circulating, RailNeos divides the lines into segments. The value of the segments, in kilometers, and their linked values of the power losses, in kW are provided. RailThermal app splits all the lines in sections. Heeding Fig. 3, it is possible to observe the representation of a line in a specific instant.

Two types of sections can appear, with no trains circulating, i.e, power losses per distance are constant, and sections in which at least one train is allocated. In these sections, the power losses by distance will be different at both sides of the train.

Fig. 3. Structure and nomenclature of a line in order to arrange the power losses by sections

The length of each section is an adaptable figure that can be changed depending on the amount of data that must be

managed. The program calculates the temperature of each section throughout the simulation. For each iteration and section, the variation of temperature is obtained and added to the temperature of the previous instant. An interface has been designed by means of Matlab's App Designer.

IV. ANALYSIS OF CONVECTIVE, RADIATED HEAT LOSS AND SOLAR HEAT GAIN OBTAINED WITH RAILTHERMAL APP

Once the method of calculation is implemented, the idea is to analyse the results provided by the tool. Evolution of convective heat loss, radiated heat loss and solar heat gain will be studied. A series of graphs will be used to compare different case studies and to draw conclusions.

A. Convective Heat Loss

The convective heat loss (q_c) have been plotted varying the section of the conductor and the coefficient K_{angle} . As can be seen in Fig.4, higher sections of the conductor means greater q_c .

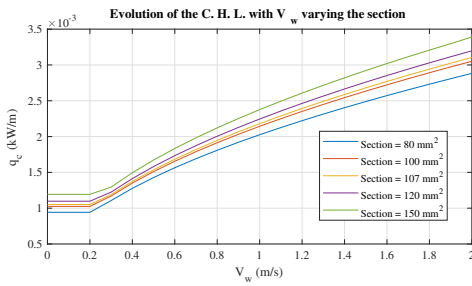


Fig. 4. Evolution of the q_c with the wind speed and changing the section of the conductor

Fig. 5 shows the influence of variable K_{angle} on q_c . This factor affects more than conductor section and H_e . Remember that this parameter is related to the angle between wind and line direction (ϕ). For values of K_{angle} close to 1 (wind direction is perpendicular to line), the heat removed by convection will be higher. For all graphs a T_s equal to 25 °C and T_∞ equal to 20 °C have been supposed.

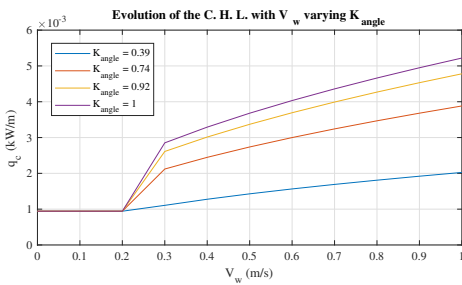


Fig. 5. Evolution of the q_c with the wind speed and changing K_{angle}

B. Radiated Heat Loss

In Fig. 6, the evolution of q_r for different sections and emissivities are presented. Note that ϵ is a characteristic of the conductor that increases over the time. As can be seen, q_r grows with ϵ and with high sections. The same temperatures for conductor and air as in convective heat loss study are used.

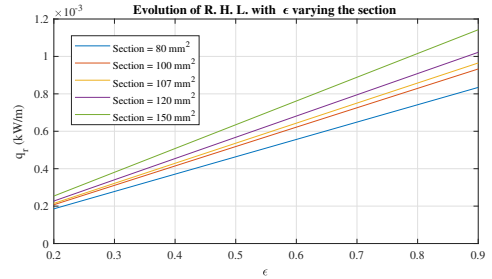


Fig. 6. Evolution of the q_r with emissivity and changing the section of the conductor

C. Solar Heat Gain

The first study compares q_s against different latitudes. In Fig. 7, the results of q_s at the summer solstice in the northern hemisphere are presented. Solar Heat Gain reaches the peak value with a Lat equal to 25°, followed by locations with Lat equal to 0° and 50°. The place in which the conductor will be exposed more time to the sun is with a Lat equal to 50°. The locations on southern hemisphere are in winter solstice, therefore their q_s are smaller. The opposite happens when the summer solstice is in the southern hemisphere.

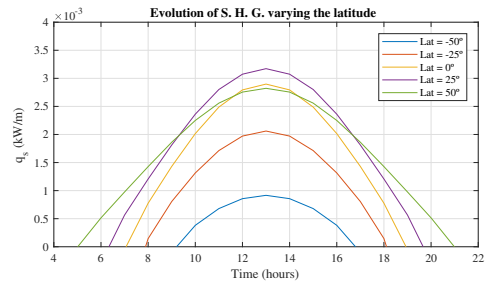


Fig. 7. Evolution of the q_s with respect the latitude. The day of the simulation is 21-July-2019 (summer solstice in the northern hemisphere)

The second case study of q_s is based on comparing the solar heat gain along the day for different dates. Heading Fig. 8, it can be observed that for dates closer to summer, solar heat gain is increasing.

The next analysis is centered on studying q_s for different α (see Fig. 9). Absorptivity is a property of the conductor. It is clearly see that for high values of α , q_s is greater. Comparing this graph with the previous ones, it is checked that variations in α affect in greater extent.

Finally, the evolution of q_s against the section of the conductor is tested. With Fig. 10, it is confirmed that for high values of the section the solar heat gain increases.

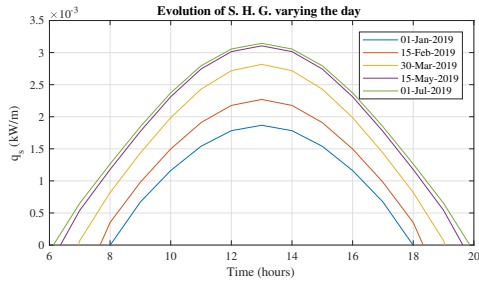


Fig. 8. Evolution of the q_s with respect day of simulation

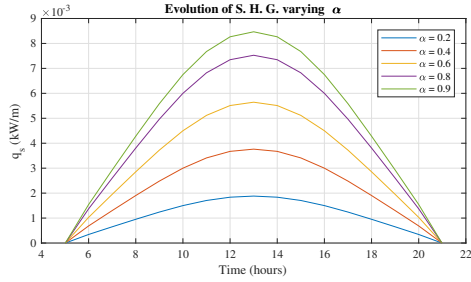


Fig. 9. Evolution of the q_s with respect absorptivity

V. INFLUENCE OF THE SECTIONING LENGTH IN THE SIMULATION TIME AND THE ERROR INCURRED

Sectioning length will affect the error incurred and the time of simulation. In this section, the main goal is to study how sectioning length changes both. In order to do that, the grid of LiÅšge's tramway was selected. The analysis will be carried out, by means of average temperature and the evolution of temperature with respect to time. Four different length of sections have been used. In order to compute the relative error of the average temperature, it is assumed the results of 25 m of section as reference.

In Fig.11, the average temperature of line 2 is presented. As can be seen, with lower sectioning length, the average temperature is more detailed.

Fig.12 has been plotted, for studying how sectioning length changes temperature from a temporal point of view. This figure shows that the highest values of temperature are reached with lowest sectioning length. Using sections of 200 m, leads to relative error between maximums of 4.8 %, i.e., 2°C. With

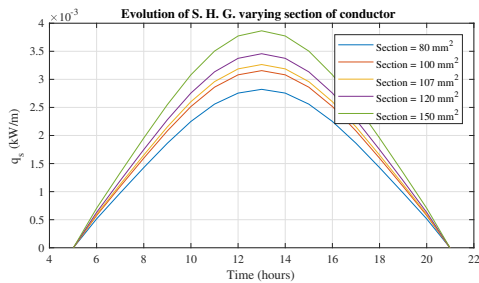


Fig. 10. Evolution of the q_s with respect section of the conductor

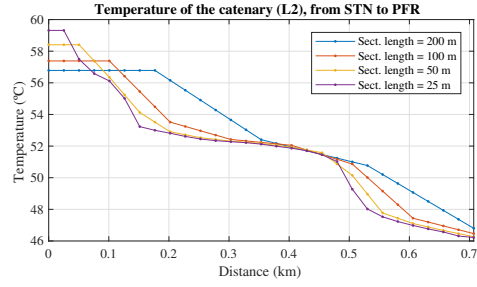


Fig. 11. Average temperature of L2 for different values of sectioning length

shorter section lengths such as 50 m, the relative error is reduced to 1.7 %

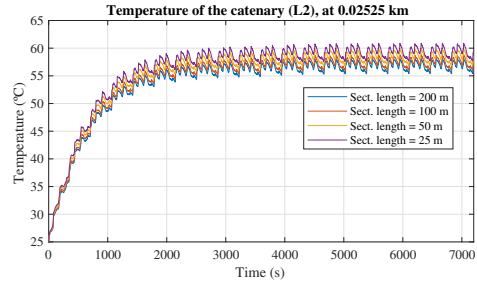


Fig. 12. Evolution of temperature, at 0.025 km of L2

Finally, a comparison between average error and simulation time has been carried out, showing that both magnitudes are inversely proportional (see Fig. 13).

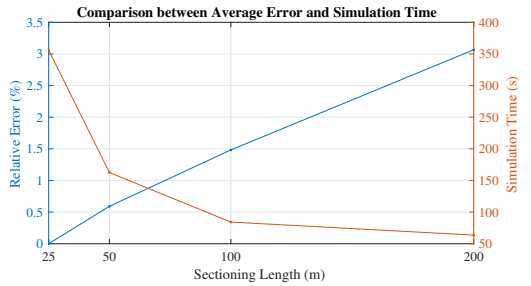


Fig. 13. Comparison between average error of Fig.11 and simulation time

VI. CASE STUDY: LIÅŠGE NETWORK

This study is focused on analyzing the thermal behavior of a tram grid in LiÅšge. The goal is to use RailThermal app to carry out a thermal study, locating the points of the lines with higher temperatures. This will allow to know which is the optimal section of the conductor.

After several iterations, the results show that with conductors of CuAg0.1 and sections of 150 mm², all points of the lines met the operation requirements. In case of Cu-ETP 150 mm², all the lines except L16, L17 and L24 fulfilled the permanent operations limits. Thus, conductors of CuAg0.1 can be installed for lines L16, L17 and L24. For the rest of the lines, Cu-ETP conductors can be used.

Fig. 14. Thermal map of LiÃšge's network with $V_w=0$ m/s and a CuAg0.1 conductor with a section of 150 mm²

TABLE II
MAXIMUM TEMPERATURE OF THE CONDUCTORS IN °C

Material	Up to 1 s	Up to 30 min	Permanent
Cu-ET	170	120	80
CuAg0.1	200	150	100
CuSn	170	130	100
CuMg0.2	170	130	100
CuMg0.5	200	150	100
ACSR/AACSR	160	-	80

In Fig. 14, 16 and 15, the final results of the grid of LiÃšge by using a CuAg0.1 conductor with 150 mm² are presented. The results show that all lines are below the operating limits (see Tab. II). In these graphs, it is indicated that no point of the network has exceeded temperatures of 100 °C, being the maximum reached in line 17, in the range of 90-100 °C.

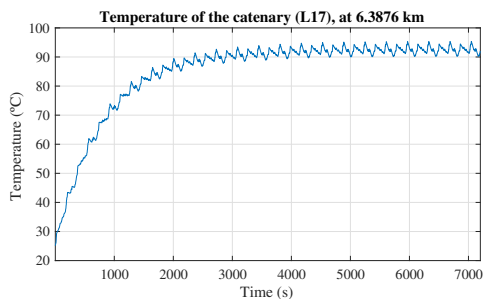


Fig. 15. Evolution of temperature for line 17, at point 6.388 km

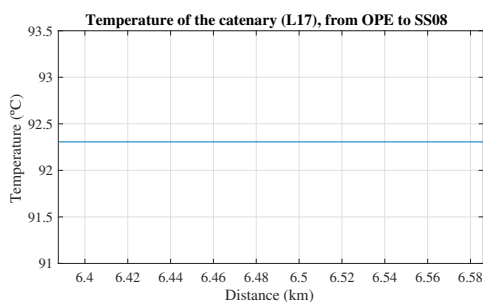


Fig. 16. Average temperature of L17

REFERENCES

- [1] A. G. Montes, "Thermal analysis in railway electrification systems," mathesis, University of Oviedo, Jun. 2019.
- [2] C. . UIC, "Rail transport and enviroment: Facts & figures," *CER/UIIC 2014*, 2015.
- [3] Y. A. Çengel and M. A. Boles, *Thermodynamics: An Engineering Approach,-PDF*. McGraw-Hill, 2008.
- [4] H. H. E. T. P. D., "Current carrying capacity of acsr." *IEEE Transactions on Power Apparatus and Systems*, pp. 1169-1178, Feb. 1958.
- [5] "Transmission conductors thermal ratings paper 68-tap-28," Report by Transmission Advisory Panel, East Central Area Reliability Coordination Agreement.

- [6] "Ieee draft standard for calculating the current-temperature relationship of bare overhead conductors," *IEEE Std 738-2012 Draft 10 (Revision of IEEE Std 738-2006)*, pp. 1-67, Sep. 2012.
- [7] W. H. McAdams, "Heat transmission, 3rd ed. new york," McGraw-Hill, 1954.
- [8] B. S. Massey and A. J. Ward-Smith, *Mechanics of Fluids: Solutions Manual*. Taylor & Francis, 2006.
- [9] D. R. Lide, *CRC handbook of chemistry and physics*. CRC press, 2004, vol. 85.
- [10] S. Murmson, "What is solar altitude?" *Sciencing*, May 2018. [Online]. Available: <https://sciencing.com/positions-stars-change-month-12761.html>
- [11] R. W. S. G. R. J. C. W. B. House, H. E., "Emissivity of weathered conductors after service in rural and industrial environments," *AIEE Transactions*, pp. 891â896, Feb. 1963.
- [12] H. H. E. Taylor, C. S., "missivity and its effects on the current carrying capacity of stranded aluminium conductors," *AIEE Transactions*, vol. 75, pt. III, pp. 970â976, Oct. 1956.